NASA Technical Memorandum 102445

Secondary Arm Coarsening and Microsegregation in Superalloy PWA-1480 Single Crystals: Effect of Low Gravity

M. Vijayakumar and S.N. Tewari
Cleveland State University
Cleveland, Ohio

and

J.E. Lee and P.A. Curreri
Marshall Space Flight Center
Huntsville, Alabama

Prepared for the
CSME Mechanical Engineering Forum 1990
sponsored by the Canadian Society for Mechanical Engineering
Toronto, Ontario, Canada, June 3-9, 1990

NASA

SECONDARY ARM COARSENING AND MICROSEGREGATION IN SUPERALLOY PWA-1480 SINGLE CRYSTALS: EFFECT OF LOW GRAVITY

M. Vijayakumar* and S.N. Tewari
Chemical Engineering Department
Cleveland State University
Cleveland, Ohio 44115

and

J.E. Lee and P.A. Curreri
National Aeronautics and Space Administration
Marshall Space Flight Center
Huntsville, Alabama 35812

Abstract

Single crystal specimens of nickel base superalloy PWA-1480 have been directionally solidified on ground and during low gravity (20 sec) and high gravity (90 sec) parabolic maneuver of KC-135 aircraft. Thermal profiles were measured during solidification by two in-situ thermocouples positioned along the sample length. The samples were quenched during either high or low gravity cycles so as to freeze the structures of the mushy zone developing under different gravity levels. Microsegregation has been measured by examining the solutal profiles on several transverse cross sections across primary dendrites along their length in the quenched mushy zone. Effect of gravity level on secondary arm coarsening kinetics and microsegregation have been investigated. The results indicate that there is no appreciable difference in the microsegregation and coarsening kinetics behavior in the specimens grown under high or low gravity. This suggests that short duration changes in gravity levels (0.02 to 1.7 g) do not influence convection in the interdendritic region. Examination of the role of natural convection, in the melt near the primary dendrite tips, on secondary arm spacings requires low gravity periods longer than presently available on KC-135. Secondary arm coarsening kinetics show a reasonable fit with the predictions from a simple analytical model proposed by Kirkwood for a binary alloy.

Introduction

An array of primary dendrites is produced during directional solidification of alloys in a positive thermal gradient, under growth conditions with large gradient of constitutional supercooling. It has been observed that the initial side-branch spacing near the tips of primary dendrites is about two to three times the dendrite tip radius (Refs. 1-3). The spacings between the neighboring side branches are observed to increase with the increasing distance from the dendrite tip. Several factors have been proposed in the literature, which may be responsible for the secondary arm coarsening. The coarsening may be due to the process of a simultaneous dissolution of smaller arms with sharper tip radii and growth of larger arms with less curvature (Refs. 4,5). It may be due to the process of dendritic separation, i.e., the secondary arm dissolving and detaching from the primary dendrite (due to the sharp curvature which reduces the local liquidus temperature) (Ref. 5). The coalescence of the neighboring side-branches can also lead to coarsening (Refs. 6,7). Measurements of the side-branch spacing from the tip of the primary dendrites to their base in the quenched mushy region of the microstructure have been used to obtain more insight into the side-branch coarsening mechanism (Refs. 2,8). Kirkwood (Ref. 8) has recently proposed a simple analytical model to predict the side-branch coarsening kinetics in binary alloys. This model is especially suited to partial directional solidification and quenching experiments.

Several recent experiments have explored the effect of gravity on primary and secondary dendrite arm spacings. Reduced gravity has generally resulted in increased secondary arm spacings (Refs. 9-12). Directionally solidified polycrystalline MAR-M246 (Ref. 7) tended to exhibit an increased secondary arm spacing in portions of the sample solidified during the low gravity maneuver of the KC-135 parabolic flight, as compared to the portion which was solidified during the high gravity. In contrast, a recent microgravity experiment on an aluminum-copper alloy has shown decreased secondary arm coarsening kinetics (Ref. 13). Long duration low gravity experiments have, by now, well established that the reduced convection causes increased primary dendrite spacings (Refs. 14,15). However, the exact mechanism by which this is brought about is not understood. It has recently been shown that the increased primary dendrite spacings observed in the low gravity grown aluminum-copper alloy sample can be explained by the primary arm spacing model due to Hunt (Ref. 16), by simply replacing the alloy growth speed, R, in the model with an order of magnitude estimate of the interdendritic fluid velocity (Ref. 15). It is generally believed that the primary and secondary spacings are controlled by the solutal profiles in the

*NASA Resident Research Associate on leave from Defence Metallurgical Research Laboratory, Hyderabad-500258, India.

melt, at the dendrite tip (G_c^t), and in the interdendritic region (G_c). Any change in G_c^t and G_c because of the gravity driven convection will affect primary dendrite spacings, their tip radii, initial side-branch spacing and secondary arm coarsening kinetics. These solutal profiles also determine the elemental microsegregation across primary dendrites produced during directional solidification. Therefore in order to understand the effect of reduced convection on the primary and secondary arm spacings, it is important to investigate its influence on the microsegregation.

The purpose of this study was to examine the effect of reduced gravity on secondary arm spacings and on the microsegregation of solutes in a multicomponent complex commercial superalloy PWA-1480. The superalloy, PWA-1480 {nominal composition, Ni-12Ta-10.4Cr-5Co-5Al-4W-1.5Ti (wt %)}, is used as a monocrystal turbine blade material in advanced gas-turbine aeroengines. This alloy was selected for this study because a preliminary investigation had shown the trend of increasing primary arm spacings to correspond with the reduced gravity periods of KC-135 parabolic flight (Ref. 17). Despite its multicomponent nature, this alloy has solidification behavior which is very similar to a binary alloy. The final solidification of PWA-1480 at the base of the primary dendrite array occurs at nearly a constant temperature (Ref. 18), similar to the isothermal eutectic solidification in a binary system. Unlike the carbon containing superalloys, such as, MAR M-246, this alloy does not have carbide precipitate formation (at a temperature between the liquidus and the eutectic temperatures) to complicate the microsegregation analysis. Since KC-135 flights are presently the only platform available to obtain the low gravity growth, the effect of gravity on the solidification behavior of this alloy was explored by directional solidification experiments during the low and high gravity periods of its maneuvers. The experiments were instrumented for in-situ temperature measurements to ensure reproducible thermal profiles. Single crystal specimens ([100] within ±8° of growth direction) were used to reduce the measurement uncertainties and scatter in the side-branch spacing and microsegregation data.

Experimental

Details of the Bridgeman type directional solidification apparatus are presented in Ref. 19. The hot zone in the furnace assembly is about 10 cm long and 1 cm in internal diameter. The water cooled copper chill zone at the bottom end of the furnace is approximately 5 cm in length. Single crystal PWA-1480 cylindrical rods ([100] within ±8° of the growth direction) were remelted in flowing argon atmosphere in alumina crucibles (0.635 cm I.D. and 46 cm long), containing two Pt- Pt 13 percent Rh thermocouples located along the specimen length with a separation of about 0.5 cm. The sample was so positioned in the furnace that approximately 5 cm length of the original 7 cm long bars was remelted. After a 20 min thermal soak the sample was directionally solidified for about 3.5 cm at growth rates in the range of 10^{-3} to 2.3×10^{-2} cm s^{-1}. When the top thermocouple was at a predetermined temperature, usually near the liquidus temperature of the alloy, 1610 K, the furnace was quickly withdrawn and the sample was quenched by spraying water on the crucible surface. Typical cooling rates of approximately 50 K s^{-1} were recorded during quench by the thermocouple located near the tips of primary dendrites. Experiments were conducted on ground and on KC-135 aircraft during its low gravity {20 sec duration, acceleration = 0.01 - 0.02 g} and high gravity (60 to 90 sec, acceleration = 1.7 g) periods of parabolic maneuvers. Flight maneuvers and quench were synchronized to obtain samples with the longest possible portion of their mushy zone solidifying during either the low gravity or the high gravity periods. Assuming that the growth speed is identical to the specimen withdrawal speed, the distances from the quenched primary dendrite tips along the specimen length were correlated with the various high and low gravity periods of the flight.

The specimens were metallographically polished and etched (etchant by volume: 33 acetic acid, 33 nitric acid, 33 water and 1 hydrofluoric acid) to correlate microstructural features, such as the tip and base of primary dendrites, with the temperatures measured by the two thermocouples. Primary dendrite spacings were measured on transverse sections (perpendicular to the growth direction) to examine their variation along the specimen length. Primary dendrite spacings reported in this paper are equal to $\sqrt{A/N}$, where A is the specimen cross-section area (transverse section) and N is the number of primary dendrites on that cross-section. Depending on the growth conditions, 200 to 600 primary dendrites were observed and counted on the corresponding specimen cross sections (18.58 to 20.14 mm^2). Secondary arm spacings were measured by averaging the distance between five adjacent side branches on the longitudinal section (parallel to the alloy growth direction) of a primary dendrite as a function of distance from the dendrite tip. Each of the side-branch spacing data reported here are the average of secondary arm spacings from four or five primary dendrites.

An Applied Research Laboratory Model SEMQ electron probe microanalyzer was used to examine the microsegregation across the primary dendrites, in the quenched interdendritic region. Because of the large amount of microprobe data required for this study, initially the ZAF (atomic number, absorption and fluorescence) corrected concentration values, obtained from the microprobe measurements, were used to prepare a calibration scheme. This calibration scheme was subsequently used for analyzing the raw microprobe data.

Results

Thermal Profile

Figure 1 shows a typical time dependence of the accelerometer, furnace position, and sample temperature data for a sample which was directionally solidified at a speed of 0.013 cm s^{-1} and quenched during the fifth high gravity parabola. The thermal profiles from the two thermocouples are also shown in this figure. The thermal gradient (G_l) in the melt at the tip of the primary dendrite array (assuming the tip temperature to be the liquidus temperature, 1610 K) was obtained from such temperature profiles.

Figure 2 shows a typical comparison of the thermal profiles (temperature versus growth distance) in the vicinity of the mushy zone, as recorded by the lower thermocouples, during two different KC-135 experiments at growth speeds of 0.013 cm s^{-1}. The specimen 1KC was quenched with its dendrite tips in the low gravity period. The other sample, 8KC, was quenched after one mushy zone length (cell length) had solidified during high gravity period of the flight. The thermal profiles of the two specimens are nearly identical. The

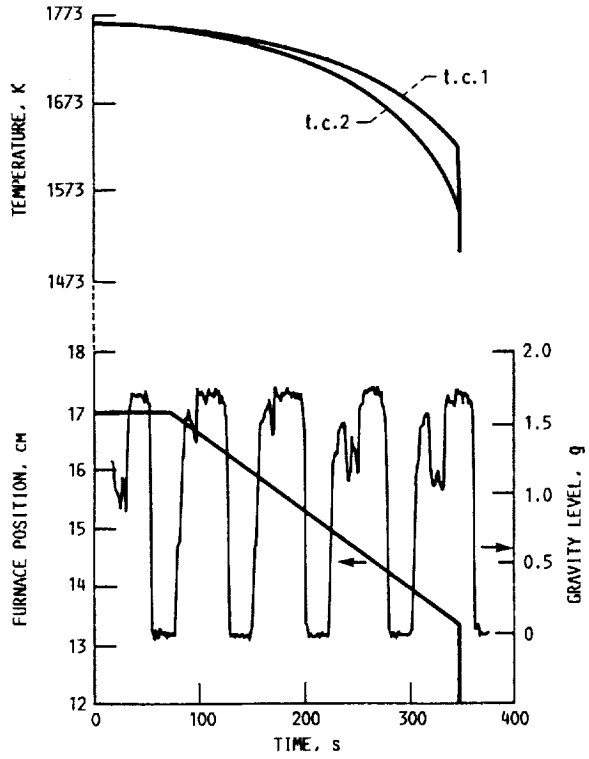

FIGURE 1. - PWA-1480 SUPERALLOY ACCELEROMETER, FURNACE POSITION, AND SAMPLE TEMPERATURE DATA FOR A SAMPLE DIRECTIONALLY SOLIDIFIED AT 0.013 cm s^{-1} DURING SEVERAL LOW AND HIGH GRAVITY MANEUVERS AND QUENCHED DURING THE FIFTH HIGH GRAVITY PARABOLA.

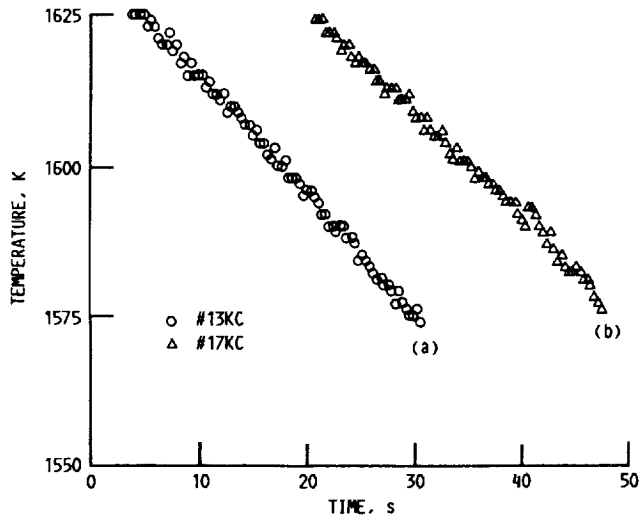

FIGURE 2. - THERMAL PROFILES NEAR THE LIQUIDUS TEMPERATURE FOR SAMPLES DIRECTIONALLY SOLIDIFIED AT 0.013 cm s^{-1} (a) SPECIMEN 13KC: G_l = 140 K cm^{-1}, QUENCHED DURING LOW GRAVITY PERIOD. (b) SPECIMEN 17KC: G_l = 150 K cm^{-1}, QUENCHED DURING HIGH GRAVITY PERIOD.

thermal gradients measured at the liquidus temperature from these plots are also similar: 140 K cm^{-1} (for 1KC) and 150 K cm^{-1} (for 8KC). The effect of gravity on the side branch coarsening kinetics will later be examined for these two samples.

Microstructure

Figure 3 shows typical longitudinal section (parallel to the growth direction) through the directionally solidified specimens. These specimens were grown at 0.013 cm s^{-1}, and have been used for examining the influence of reduced gravity on microsegregation. They show the well aligned primary dendrites in the mushy zone. The dendrite tips and the quenched liquid ahead of the tips can be clearly seen in these microstructures. A distinct change in the microstructure of the quenched interdendritic region, observed at a temperature corresponding to about 1550 K (Ref. 18), was used to locate the base of the primary dendrite array, where the last interdendritic liquid solidified just before quench. The specimen growth speed (assumed to be same as the furnace withdrawal speed) and the cell length data have been used to obtain the corresponding coarsening time for the side-branches located at any given distance from the dendrite tip. In Fig. 3, the portions in the mushy zone which solidified during high-g and low-g periods are marked accordingly.

Steady State Growth: Figure 4 plots the variation in primary dendrite spacings along the directionally solidified length of a specimen grown at 0.013 cm s^{-1} (13KC). Distance "A" marked in this figure indicates the cell length. The quenched primary dendrite tips are schematically shown on the right hand side. Start of directional solidification is on the left side. This figure shows that initially the primary dendrite spacings decrease along the length of the solidifying specimens before becoming almost constant. A steady-state solidification can therefore be assumed to occur after growth of about 1 cm of the specimen length. Nearly steady-state growth conditions are subsequently achieved for a length which is approximately equal to two to three times the cell length, before the sample is finally quenched.

Effect of Gravity

Side-Branch Coarsening Kinetics: Figure 5 shows the secondary arm spacing versus time (distance from the dendrite tip divided by growth speed) plots for specimens which were grown during KC-135 flights at 0.013 cm s^{-1} respectively. The high gravity (g_h) and low gravity (g_l) periods are also marked in these figures. The portions near the quenched end, showing the increasing secondary arm spacings from the tips of primary dendrite, along the cell length, can be used to obtain the side-branch coarsening kinetics. The cell lengths observed in these specimens are schematically shown in these figures (lower right). For the growth rate, 0.013 cm s^{-1} (Fig. 5(a)), even the entire period of low gravity (approximately 20 sec) is not sufficient to obtain the growth of one complete length of the primary dendrite array (cell length = 0.48 cm). Due to the experimental difficulty of being able to achieve an exact synchronization among crucible withdrawal, flight maneuver and quenching, and the need to ensure the reproducible thermal profiles near the mushy zone, it was not possible to obtain specimens with one complete cell length forming during the low gravity period. On the other hand, the high gravity period (about 45 sec) is sufficient to obtain the side-branch coarsening along the entire length of the primary dendrite, Fig. 5(b).

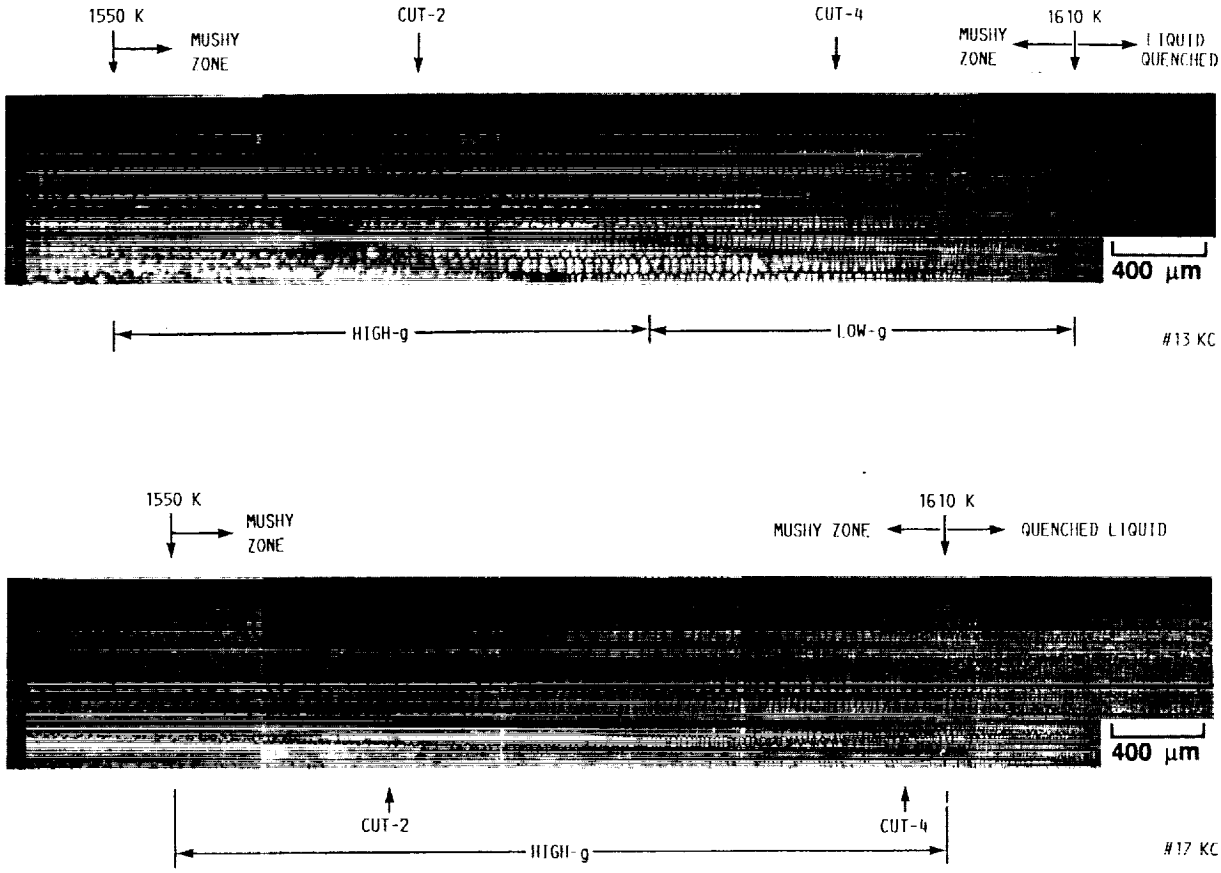

FIGURE 3. - LONGITUDINAL MICROSTRUCTURES SHOWING THE ALIGNED PRIMARY DENDRITES IN THE QUENCHED MUSHY ZONE FOR SPECIMENS GROWN AT 0.013 cm s^{-1}. THE TEMPERATURES AT THE TIP (1610 K) AND THE BASE (1550 K) ARE INDICATED. LOW-g AND HIGH-g REGIONS ARE MARKED FOR 13KC. FOR 17KC, WHOLE MUSHY ZONE HAS DEVELOPED UNDER HIGH-g. TRANSVERSE SECTIONS ON WHICH MICROSEGREGATIONS WERE ANALYZED ARE INDICATED BY CUT-2 AND CUT-4.

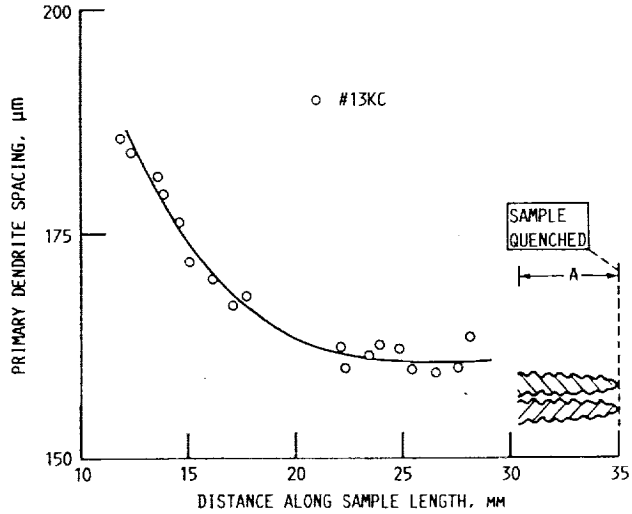

FIGURE 4. - VARIATION OF PRIMARY DENDERITE SPACINGS ALONG THE LENGTH OF A SPECIMEN, SOLIDIFIED AT 0.013 cm s^{-1} (13KC). THE DISTANCE MARKED 'A' IS THE EXPERIMENTALLY OBSERVED CELL LENGTH. PRIMARY DENDRITES SHOW REASONABLY CONSTANT SPACINGS FOR A DISTANCE SLIGHTLY MORE THAN TWICE THE CELL LENGTH NEAR THE END WITH THE QUENCHED DENDRITE TIPS.

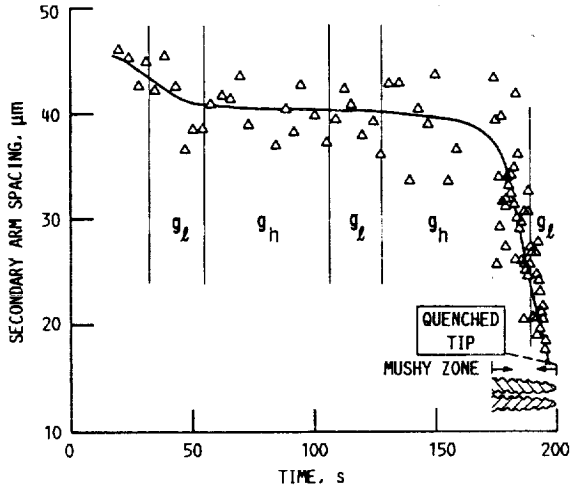

(a) SAMPLE QUENCHED DURING LOW GRAVITY.

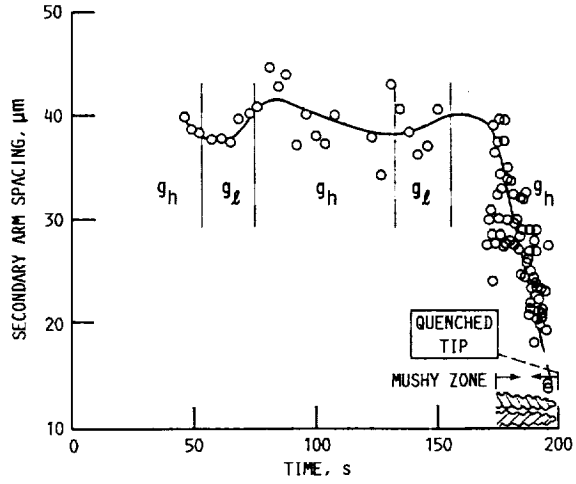

(b) SAMPLE QUENCHED DURING HIGH GRAVITY.

FIGURE 5. - SECONDARY ARM SPACING VERSUS TIME PLOTS FOR SUPERALLOY SPECIMENS DIRECTIONALLY SOLIDIFIED AT 0.013 cm s^{-1}. APPROXIMATE AVERAGE BEHAVIOR IS SHOWN BY THE SOLID LINES. THE HIGH GRAVITY AND LOW GRAVITY PERIODS ARE MARKED IN THESE FIGURES. THE CELL LENGTH IN THE MUSHY ZONE IS ALSO SCHEMATICALLY SHOWN.

Figure 5 shows that there is a large scatter in the data. The approximate average behavior is shown by the solid lines in these figures. The secondary arm spacings do not show an increase corresponding to the transitions from high gravity to low gravity, as has been earlier reported in another directionally solidified superalloy, Mar M-246 (Ref. 9).

The initial data in Figs. 5(a) and (b) have been replotted for the two specimens grown at 0.013 cm s^{-1} in Fig. 6, as side-branch spacing versus coarsening time. Within the experimental scatter, the secondary arm coarsening kinetics appear to be the same for the high gravity and the low gravity periods. However, there is a large scatter in the data. The scatter in the side-branch spacing data was observed to decrease with the decreasing growth speeds.

Microsegregation: Figure 7 shows a typical transverse section (Fig. 7(a)) and the corresponding solute profiles (Fig. 7(b)), starting from the interdendritic eutectic region at one end and terminating at the interdendritic eutectic region at the opposite end. For tantalum, aluminum and titanium the solute contents increase from the core of the primary dendrite towards its periphery. This is the behavior expected for solutes with partition coefficients less than one. It is interesting to note that the nickel based binaries for these three solutes have partition coefficients less than one (Ref. 20). On the other hand cobalt and tungsten, with their partition coefficients based on nickel based binaries greater than one, show an opposite trend. Their solute contents decrease in going from the core of the dendrite cross section to its periphery. Chromium showed a reasonably uniform distribution across the primary dendrite and has not been studied in detail in this investigation. Solutal profiles such as these have been folded with respect to the center point "O" (Fig. 7(a)) and the distance information converted to fraction solid using the relation: fraction solid, $f_s = \{x/d_o\}^2$, where x is the distance along OA or OB, and d_o is half the average distance (similar to AB in Fig. 7(a)) for the transverse section, just below the base of the primary dendrite array in the quenched mushy zone. Typically three to four dendrites were analyzed and the concentration data averaged over a f_s range of 1 percent.

Figure 8 shows the optical micrographs of the transverse microstructures for specimens, 13KC and 17KC, whose longitudinal microstructures were shown in Fig. 3. Figures 8(a) and (b) correspond to sections which solidified in high-g (Cut 2 in Fig. 3). Figures 8(c) and (d) are for portions solidified in low-g for 13KC and in high-g for 17KC (Cut 4 in Fig. 3). Microsegregation profiles for tantalum and tungsten corresponding to these micrographs are presented in Fig. 9. The scatter in the composition data is minimal near the tips of primary dendrite, as is evidenced by

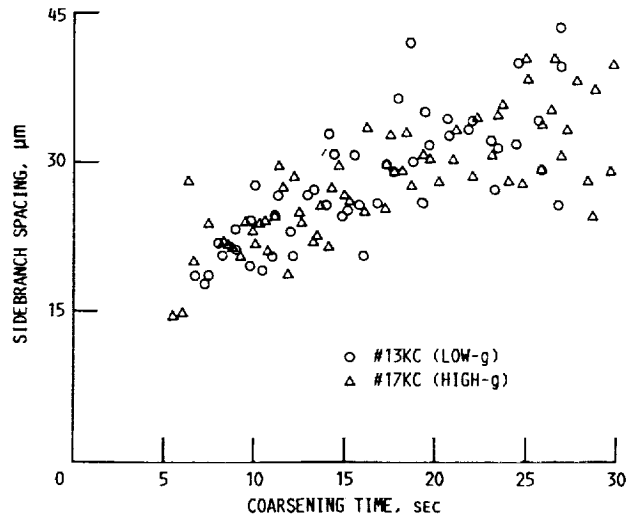

FIGURE 6. - COMPARISON OF THE SIDE-BRANCH COARSENING KINETICS DURING DIRECTIONAL SOLIDIFICATION (GROWTH SPEED 0.013 cm s^{-1}) OF SUPERALLOY PWA-1480 IN THE LOW GRAVITY AND HIGH GRAVITY PERIODS OF THE PARABOLIC FLIGHT. CONSIDERING THE SCATTER IN THE DATA, ANY INFLUENCE OF GRAVITY ON THE SECONDARY ARM COARSENING KINETICS IS NOT RESOLVABLE.

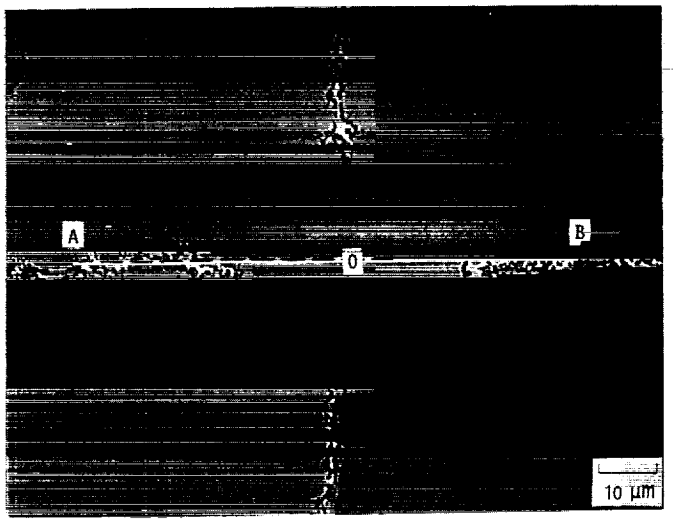

(a) BACKSCATTERED ELECTRON IMAGE (17KC) SHOWING THE PATH OF THE ELECTRON BEAM DURING ELECTRON PROBE MICROANALYSIS.

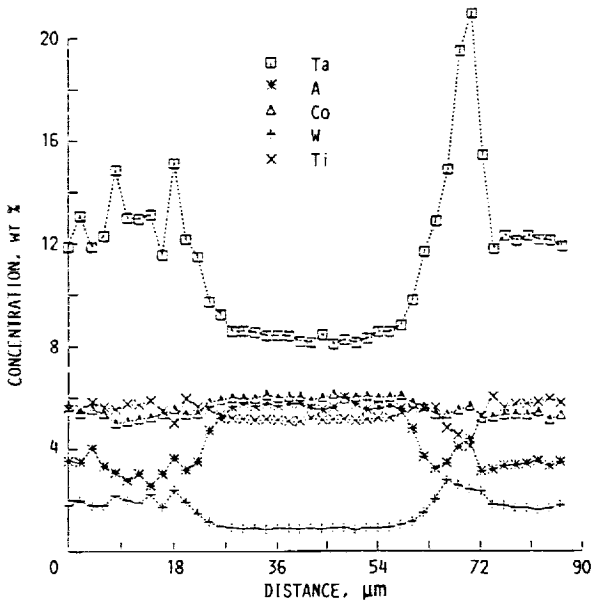

(b) TYPICAL CONCENTRATION PROFILES FOR VARIOUS SOLUTE ELEMENTS ALONG THE PATH IN (a) ABOVE.

FIGURE 7. - SOLUTAL DISTRIBUTIONS ACROSS PRIMARY DENDRITE.

about 3 percent scatter in the composition data closer to zero fraction solid (Fig. 9). It is however quite large (10 to 20 percent) in the quenched interdendritic liquid region of the microstructure. Here, the microstructure consists of discrete particles of γ and γ' phases, with very different compositions. The relatively large scatter in the composition profile (10 to 20 percent) is generated as the electron microprobe beam traverses these γ and γ' phases. Figure 9 shows that the profiles for both the sections superimpose on each other irrespective of the gravity levels in which they solidified. It suggests that the change in gravity level has not influenced the microsegregation pattern for the two solutes. Similar behavior (not reported here) was observed for all other solutes. Since the microsegregation profiles, as shown in Fig. 9, represent the solutal profiles in the interdendritic melt during growth, the above observations establish that the changing gravity levels, which occurs during parabolic flights of KC-135 aircraft, have no effect on the solute profiles in the interdendritic melt.

It is clear from Fig. 9 that the solute contents in the dendrite core (near zero fraction solid) are nearly the same for the transverse sections examined in the mushy zone. This indicates that the solid-state diffusion effects are negligible. In the presence of significant diffusion in the solid, the solute content at zero fraction solid will be expected to be higher on a transverse section closer to the base of the primary dendrite, as compared to that near the tip, for solutes having less than unity partition coefficients (Ta, Ti, and Al). Opposite would be the case for W and Co.

Discussion

Comparison of Side-Branch Coarsening Behavior with Theoretical Model: Kirkwood (Ref. 8) has recently presented proposed a simple analytical model to predict the side-branch coarsening kinetics in binary alloys. This model is especially suited to partial directional solidification and quenching experiments. It assumes a constant temperature and composition of the interdendritic melt. It treats the coarsening process as simultaneous dissolution of smaller arms (spheres) with sharper tip radii and growth of larger arms with less curvature. The model predicts the following behavior,

$$d^3 = -\{128\ \sigma\ D_l\ T/m_l\ C_o\ (k - 1)\ H\}t \qquad (1)$$

where, d is the side-branch spacing corresponding to the coarsening time t, D_l, the solute diffusivity in the melt, σ, the liquid-solid surface energy, m_l, the liquidus slope, C_o, the solute content of the alloy, k, the solute partition coefficient and H/T is the entropy of fusion per unit volume. The experimentally observed coarsening behavior for superalloy PWA-1480 is compared below with prediction from the above relationship, treating the multicomponent superalloy as if it were a binary.

Figure 10 plots $\log_{10}(d)$ versus $\log_{10}(t)$ data obtained from several experiments. It contains the data from several specimens, grown at 0.001 to 0.023 cm s^{-1}, both on ground and on KC-135. The straight line drawn through the data is the linear least squared fit given as,

$$\log_{10}(d, \mu m) = (1.021 \pm 0.014) + (0.325 \pm 0.001) \times \log_{10}(t, sec)$$

For this fit, the correlation coefficient is 0.825 and the relative standard deviation is 5.2 percent. The slope of this line, 0.325, is same as that expected from the above coarsening relationship, Eq. 1. The experimentally obtained value, 1.2×10^{-9} cm^3 s^{-1} of the terms in the bracket in Eq. 1 (obtained from the intercept on the Y-axis in Fig. 10), will now be used to obtain the expected D_l/k value for PWA-1480 in the following manner. The terms within the bracket can also be expressed as, $\{128\ (\sigma/H)\ (T/T_o)\ (D_l/k)\}$, where $T_o = m_l C_o (k - 1)/k$ is the freezing range of the alloy (1610 K, liquidus and 1575 K, solidus). We will assume the σ and H value for PWA-1480 to be the same as for nickel, 255 erg cm^{-2} (Ref. 21) and 2.77×10^{10} erg cm^{-3} (Ref. 22) respectively. We will assume the coarsening temperature, T, to be the liquidus temperature, 1610 K. The (D_l/k) value thus obtained by fitting the above

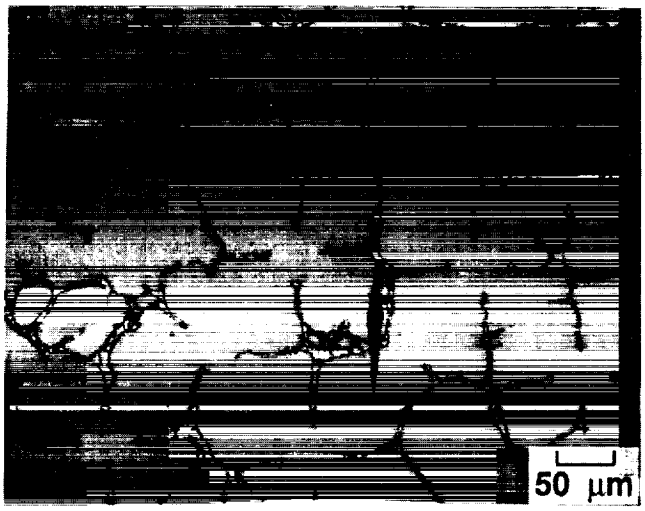

(a) CUT-2 FOR 13KC.

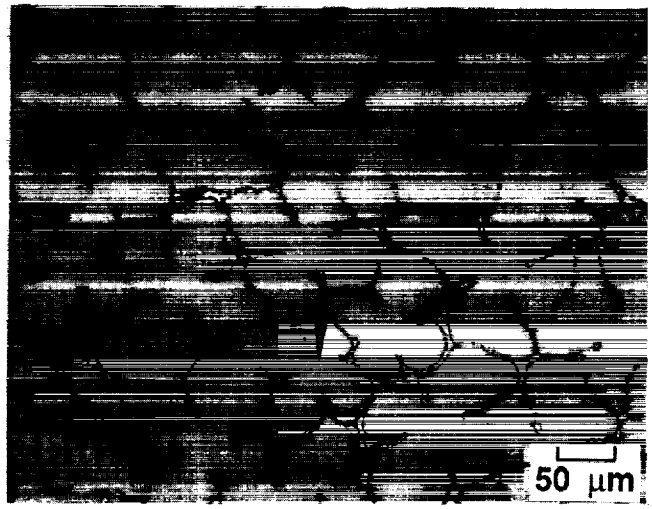

(b) CUT-2 FOR 17KC.

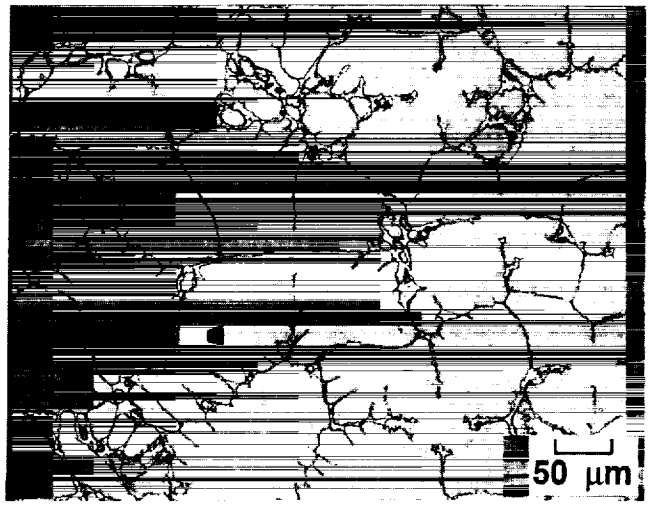

(c) CUT-4 FOR 13KC.

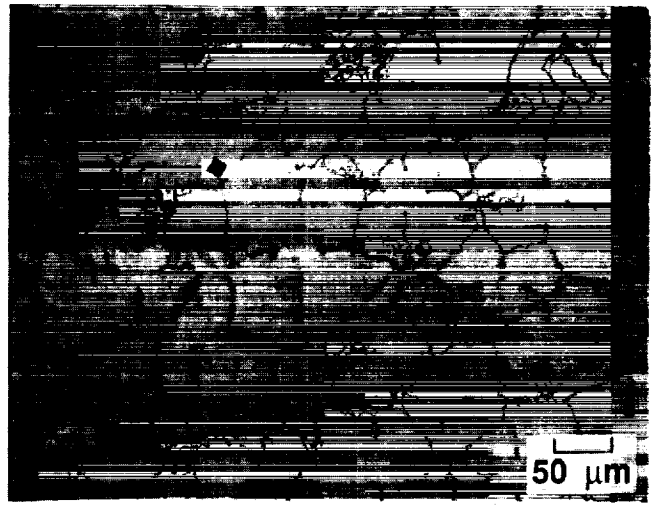

(d) CUT-4 FOR 17KC.

FIGURE 8. - TRANSVERSE MICROSTRUCTURES USED IN EXAMINING THE INFLUENCE OF GRAVITY LEVELS ON MICROSEGREGATION. (a), (b) AND (d) ARE FOR THE PORTIONS WHICH SOLIDIFIED IN HIGH-g. (c) IS FOR THE PORTION SOLIDIFIED IN LOW-g.

mentioned coarsening relationship to the experimental data is about 2×10^{-5} cm^2 s^{-1}. The experimentally observed partition coefficients for the various solutes in superalloy PWA-1480 are in the range from 0.4 to 1.7 (Ref. 18). Thus the solute diffusivity in the PWA-1480 melt (D_l) would be predicted to be in the range from 0.8 to 3.4×10^{-5} cm^2 s^{-1}. This is in a reasonable agreement with reported solutal diffusivity, about 2 to 8×10^{-5} cm^2 s^{-1} (Ref. 23), obtained from the estimations based on the use of the constitutional supercooling criterion for plain front solidification of several superalloys.

Need for Long-time Low Gravity Experiments: It has recently been shown (Ref. 24) that the time required (t_r) to reach a certain fraction of final steady-state fluid velocity value (FR), after a change in gravity level, is approximately equal to $-0.029 \ln(1-FR)\, r^2/\mu$, where r is the radius of the crucible and μ is the kinematic viscosity. For a viscosity of 6.1×10^{-3} cm^2 s^{-1} (for nickel melt at its melting point, Ref. 25), and the crucible radius of 0.32 cm, about 2 sec will be required to reach the 99 percent fraction of the steady-state fluid velocities after any change in gravity. This suggests that during the parabolic maneuvers of the KC-135 flight, growth conditions were obtained where the convection in the melt was suppressed for about 18 sec. Similarly during the high-g portions of the flight, the increased convection in the melt was available for about 88 sec. Because of the very small dimensions of the interdendritic melt, much smaller than the primary arm spacings, 150 μm, the changed gravity effects will be felt by the interdendritic melt in times much shorter than 2 sec.

The final secondary arm spacings observed at the base of the primary dendrites in an array depend on the following factors:

(1) The initial side branch spacing near the tips of primary dendrite array: This spacing is known to linearly scale with the tip radius (Refs. 1-3). The

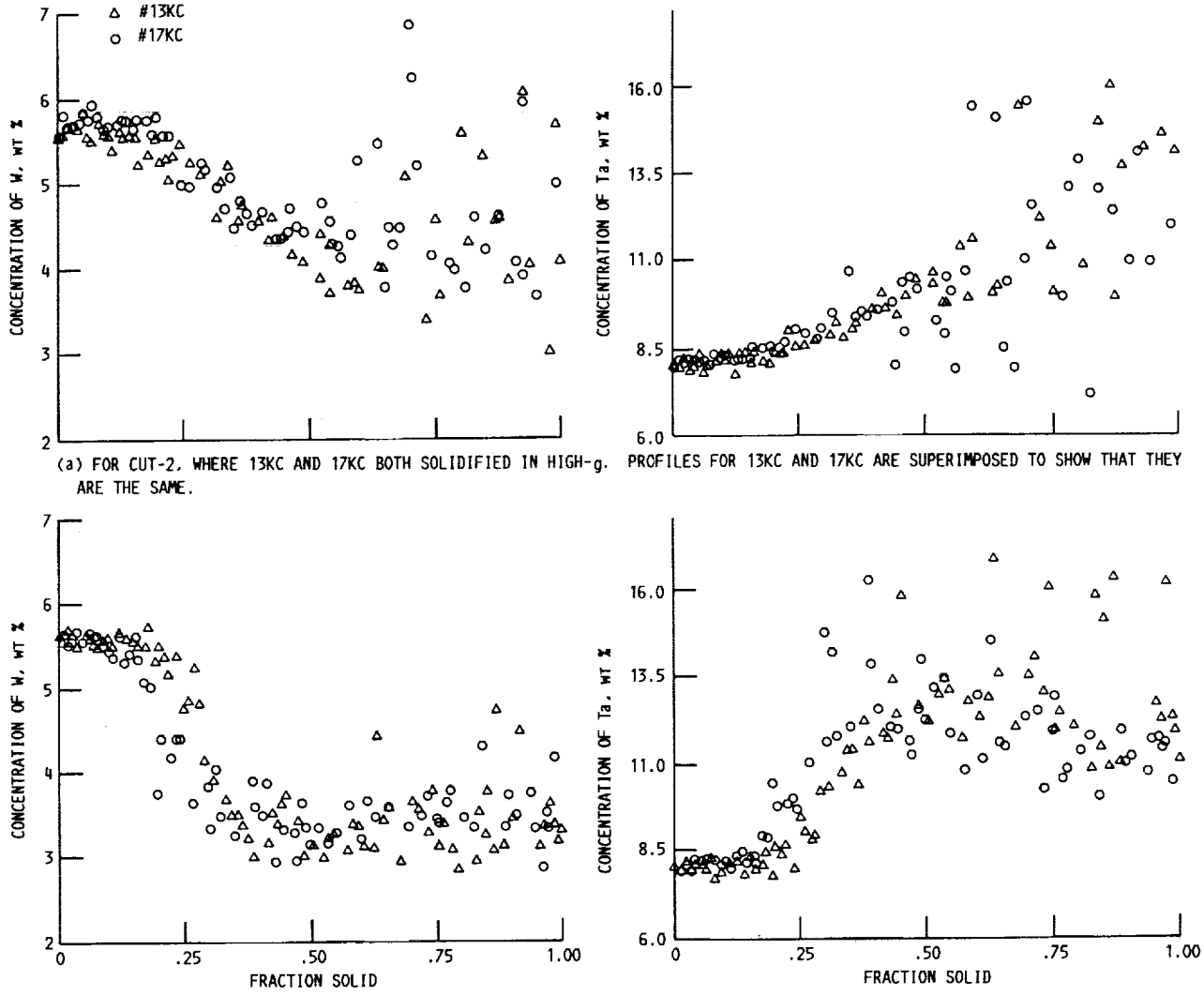

(a) FOR CUT-2, WHERE 13KC AND 17KC BOTH SOLIDIFIED IN HIGH-g. PROFILES FOR 13KC AND 17KC ARE SUPERIMPOSED TO SHOW THAT THEY ARE THE SAME.

(b) FOR CUT-4, WHERE 13KC HAS SOLIDIFIED IN LOW-g AND 17KC IN HIGH-g. NO DISCERNABLE DIFFERENCES EXIST BETWEEN THE TWO PROFILES.

FIGURE 9. - EFFECT OF GRAVITY LEVELS ON MICROSEGREGATION OF Ta AND W.

tip radius is determined by the solutal profile in the melt at the dendrite tips. Convection in the melt is expected to influence this solutal profile in the melt at the dendrite tips. The solutal build up in the melt at the tips (for $k < 1$) increases with decreasing growth speed. Influence of reduced convection on this solutal profile requires low-g and high-g experiments at growth speeds much slower than available on KC-135.

(2) The side-branch coarsening kinetics: This will be a function of convection in the interdendritic melt and the interdendritic solutal profiles. Comparison of specimen portions grown during low-g and high-g periods of the KC-135 parabolic flight, for their side-branch coarsening (Fig. 6) and interdendritic solute profile (microsegregation, Fig. 9) behavior, suggests that these are not influenced by the gravity levels examined in this study. However, for both of these, there is a large scatter in the experimental data.

(3) The coalescence of neighboring side-branches: The coalescence of neighboring side-branches is expected to be significant only in the interdendritic regions closer to the base of the primary dendrites. The coalescence process will be influenced by factors, such as, interdendritic precipitates, primary arm spacings, volume fraction of interdendritic melt, etc. As mentioned earlier, PWA-1480 does not have the complexity arising from the interdendritic precipitation. Since the interdendritic channels are very narrow near the base of the primary dendrites the coalescence process is not expected to be influenced by the changing gravity levels. This effect has not been investigated in this research.

The scatter in a plot, such as Fig. 9, depends on several factors, the microprobe measurement process (instrumental scatter), the scatter due to local microstructural inhomogeneities larger than the probe x-ray resolution (approximately 3 μm), problem of imperfect alignment of the primary dendrites with the growth direction, and the statistical variation in the primary dendrite arm size. The relative standard deviation of the concentration values, caused by the fluctuations

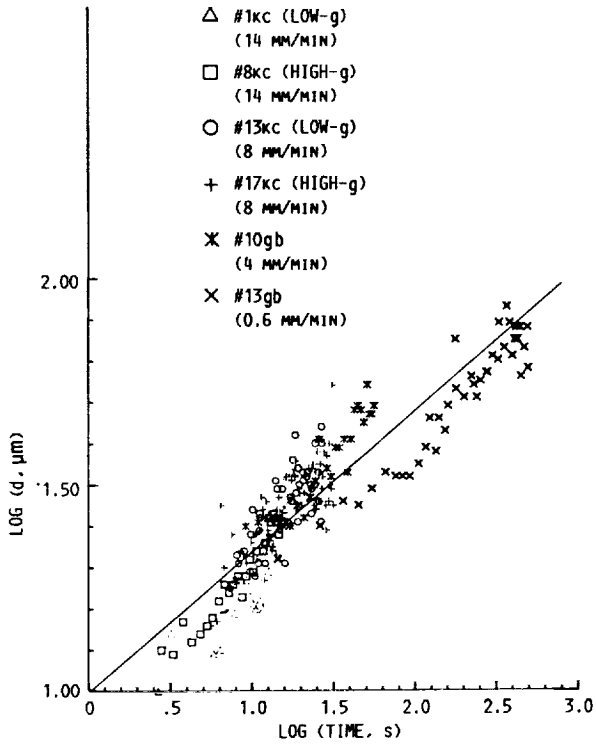

FIGURE 10. - SIDE-BRANCH COARSENING KINETICS IN SUPERALLOY, PWA-1480. THE LINE IS THE LINEAR LEAST SQUARED FIT THROUGH THE DATA. THE SOLUTAL DIFFUSIVITY VALUES EXTRACTED FROM THIS PLOT, ASSUMING THE SIDE-BRANCH COARSENING KINETICS TO OBEY THE SIMPLE ANALYTICAL MODEL PROPOSED BY KIRKWOOD (REF. 8) FOR A BINARY ALLOY, ARE IN REASONABLE AGREEMENT WITH THE LITERATURE REPORTED VALUES.

in the instrument settings and the statistical nature of the x-ray counting process, is about ±3 percent (Ref. 18). The scatter due to the local microstructural variations within the primary dendrite is minimal, as is evidenced by about 3 percent scatter in the composition data closer to zero fraction solid (Fig. 9). The major sources of scatter in the microsegregation, across the primary dendrites, are the variations in the primary arm size and its nonalignment with the growth direction. A perfect alignment would result in a fourfold symmetry in the transverse microstructure of the dendrites. This would result in a symmetrical solute distribution along the opposite sides of the dendrite core along "A" type paths (as shown in Fig. 7). Otherwise the solute content at a given distance from the dendrite core on one side would be different from the one at the same distance on the opposite side, causing the scatter in the solute concentration versus fraction solid (fraction distance) plots. Contribution from this scatter would be zero at the dendrite core, and would increase with the increasing distance from the core. The scatter would be further enhanced when the data obtained from several primary dendrites with different alignments are superimposed. The fourth kind of scatter, due to the differences in the primary arm spacings, results from the errors in the fraction solid value calculated based on the average spacing near the eutectic isotherm, as has been done in this study. The variation in the primary dendrite spacing in the directionally solidified superalloy PWA-1480 specimens is about 10 percent.

During ground based experiments it has been observed that the scatter in the side-branch spacing data decreases considerably with the decreasing growth speed. The lower growth speeds will also make it possible to examine the side-branch coarsening kinetics over a much longer time period. However, the low gravity period of KC-135 parabolic flight is already too short, for solidifying even one complete length of dendrite array, at a growth speed of 0.013 cm s^{-1}. Longer time, low-gravity partial directional solidification and quenching experiments, required for a better resolution of the influence of reduced gravity, are not possible on KC-135. Such experiments can be carried out in the low gravity environment provided by the space shuttle. Because of the absence of cycling gravity levels, such experiments at low gravity will produce a more regular dendrite array, than the specimens examined in this study. This will further reduce the scatter in the side-branch coarsening and microsegregation data.

Specimens grown at much slower growth speed (approximately 0.001 cm s^{-1}) than examined in this study, in the low gravity environment of space, can help us isolate the effect of reduced gravity on the convection in the interdendritic melt and in the melt ahead of the dendrite array.

Conclusions

Following conclusions can be drawn from this study on single crystal superalloy, PWA-1480, specimens directionally solidified on ground and during low gravity (20 sec) and high gravity (60 to 90 sec) periods obtained during parabolic maneuvers of KC-135 aircraft. These specimens were rapidly quenched after partial solidification to retain the mushy-zone microstructure and the solutal distributions.

1. The specimen length which can be solidified during low gravity time available from the KC-135 flights is much smaller than mushy zone length of PWA-1480. Because of the insufficient low gravity time, no definite conclusions can be drawn about the effect of gravity on the secondary arm spacing.

2. Side-branch coarsening kinetics and the solutal profiles in the interdendritic melt are not significantly influenced by the gravity levels examined here, 0.01 to 1.7 g. This is considered reasonable because the array of closely spaced primary dendrites effectively dampens the convection in the interdendritic region. Experiments at growth speeds less than about 0.001 cm s^{-1}, to obtain about three to four times the cell length directionally solidified in low gravity, are required to draw definite conclusions about the effect of reduced convection in the melt ahead of primary dendrite tips, on the secondary arm spacings. These experiments are feasible only in the long duration microgravity environment of space.

3. Measurement of the side-branch spacing along the length of the primary dendrites, from their quenched tip to their base, shows that the secondary arm coarsening kinetics in PWA-1480 are in a reasonable agreement with the behavior expected from the simple analytical model of Kirkwood (Ref. 8), developed for binary alloys.

Acknowledgment

This work was funded by the Marshall Space Flight Center, Center Director's Discretionary Fund,

CDDF-87-14, under a cooperative agreement (NAG8-091). Research facilities in the Microgravity Materials Science Laboratory, NASA Lewis Research Center, Cleveland, were used during this study. Appreciation is expressed to R.E. Shurney of Marshall Space Flight Center; G. Workman, and R. Bond of University of Alabama in Huntsville; and the personnel of Johnson Space Center who operate the KC-135.

References

1. Somboonsuk, K., Mason, J.T., and Trivedi, R., "Dendritic Spacing: Part I. Experimental Studies," Metallurgical Transactions A, Vol. 15, No. 6, pp. 967-975, 1984.

2. Tewari, S.N., Nesarikar, V.V., and Lee, D., "Side-Branch Morphology and Coarsening in Directionally Solidified Pb-8.4 at% Au," (to appear in Metallurgical Transactions A).

3. Huang, S.C., and Glicksman, M.E., "Fundamentals of Dendritic Solidification - I. Steady-State Tip Growth," Acta Metallurgica, Vol. 29, No. 10, pp. 701-711, 1981.

4. Kattamis, T.Z., Coughlin, J.C., and Flemings, M.C., "Influence of Coarsening on Dendrite Arm Spacing of Aluminum-Copper Alloys," Transactions of the American Institute of Metallurgical Engineers, Vol. 239, No. 10, pp. 1504-1511, 1967.

5. Kahlweit, M., "On the Ageing of Dendrites," Scripta Metallurgica, Vol. 2, pp. 251-254, 1968.

6. Young, K.P., and Kirkwood, D.H., "The Dendrite Arm Spacings of Aluminum-Copper Alloys Solidified Under Steady-State Conditions," Metallurgical Transactions A, Vol. 6, No. 1, pp. 197-205, 1975.

7. Curreri, P.A., Lee, J.E., and Stefanescu, D.M., "Dendritic Solidification of Alloys in Low Gravity," Metallurgical Transactions A, Vol. 19, No. 11, pp. 2671-2676, 1988.

8. Kirkwood, D.H., "A Simple Model for Dendrite Arm Coarsening During Solidification," Materials Science and Engineering, Vol. 73, pp. L1-L4, 1985.

9. Johnston, M.H., Curreri, P.A., Parr, R.A., and Alter, W.S., "Superalloy Microstructural Variations Induced by Gravity Level During Directional Solidification," Metallurgical Transactions A, Vol. 16, No. 9, 1683-1687, 1985.

10. Johnston, M.H., and Griner, C.S., "The Direct Observation of Solidification as a Function of Gravity Level," Metallurgical Transactions A, Vol. 8, No. 1, pp. 77-82, 1977.

11. Johnston, M.H., and Parr, R.A., "The Influence of Acceleration Forces on Dendritic Growth and Grain Structure," Metallurgical Transactions B, Vol. 13, No. 1, pp. 85-90, 1982.

12. Stefanescu, D.M., Curreri, P.A., and Fiske, M.R., "Microstructural Variations Induced by Gravity Level During Directional Solidification of Near-Eutectic Iron-Carbon Type Alloys," Metallurgical Transactions A, Vol. 17, pp. 1121-1130, 1986.

13. Tensi, H.M., and Schmidt, J.J., "Influence of Thermal Gravitational Convection on Solidification Processes," Scientific Results of the German Spacelab Mission D1, P.R. Sahm, R. Jensen, and M.H. Keller, eds., 1987, pp. 216-222, DFVLR, Federal Republic of Germany.

14. Favier, J.J., Berthier, J., Arragon, Ph., Malmejac, Y., Khryapov, V.T., and Barmin, I.V., "Solid/Liquid Interface Stability in Normal and Microgravity Conditions: The Elma 01 Experiments," Acta Astronautica, Vol. 9, No. 4, pp. 255-259, 1982.

15. Dupouy, M.D., Camel, D., and Favier, J.J., "Natural Convection in Directional Dendritic Solidification of Metallic Alloys - I. Macroscopic Effects," Acta Metallurgica, Vol. 37, No. 4, pp. 1143-1157, 1989.

16. Hunt, J.D., Solidification and Casting of Metals, 1979, pp. 3-9, The Metals Society, London.

17. McKay, M.H., Lee, J.E., and Curreri, P., "The Effect of Gravity Level on the Average Primary Dendritic Spacing of a Directionally Solidifed Superalloy," Metallurgical Transactions A, Vol. 17, No. 12, pp. 2301-2303, 1986.

18. Tewari, S.N., Vijayakumar, M., Lee, J.E., and Curreri, P.A., "Microsegregation in Directionally Solidified Nickel Based Superalloy, PWA-1480, Single Crystal," (Submitted to Metallurgical Transactions A).

19. Smith, G.A., and Workman, G., "Operational Procedure and Specification for the KC-135 Automatic Directional Solidification Furnace Reference," NASA Contract Report NAS8-34530, 1985.

20. Metals Handbook, Vol. 8, 8th Edition, 1973, pp. 262,258,291,326, American Society for Metals, Metals Park, OH.

21. Holloman, J.H., and Turnbull, D., "Nucleation," Progress in Metal Physics, Vol. 4, pp. 333-388, 1953.

22. Geiger, G.H., and Poirier, D.R., Transport Phenomena in Metallurgy, 1972, p. 580, Addison Wesley, Reading, MA.

23. Quested, P.N., and McLean, M., "Solidification Morphologies in Directionally Solidified Superalloys," Materials Science and Engineering, Vol. 65, pp. 171-180, 1984.

24. Chait, A., and Arnold, W.A., "Residual Acceleration Effects in Directional Solidification in Various Low-g Environments," presented at the American Society for Metals World Materials Congress, Chicago, IL, Sept. 24-30, 1988.

25. Battezzati, L., and Greer, A.L., "The Viscosity of Liquid Metals and Alloys," Acta Metallurgica, Vol. 37, No. 7, pp. 1791-1802, 1989.

NASA
National Aeronautics and Space Administration

Report Documentation Page

1. Report No.	2. Government Accession No.	3. Recipient's Catalog No.
NASA TM-102445		

4. Title and Subtitle	5. Report Date
Secondary Arm Coarsening and Microsegregation in Superalloy PWA-1480 Single Crystals: Effect of Low Gravity	January 1990
	6. Performing Organization Code

7. Author(s)	8. Performing Organization Report No.
M. Vijayakumar, S.N. Tewari, J.E. Lee, and P.A. Curreri	E-5220
	10. Work Unit No. 647-27-05

9. Performing Organization Name and Address	11. Contract or Grant No.
National Aeronautics and Space Administration Lewis Research Center Cleveland, Ohio 44135-3191	
	13. Type of Report and Period Covered Technical Memorandum
12. Sponsoring Agency Name and Address	14. Sponsoring Agency Code
National Aeronautics and Space Administration Washington, D.C. 20546-0001	

15. Supplementary Notes

Portions of this paper were presented at the CSME Mechanical Engineering Forum 1990, sponsored by the Canadian Society for Mechanical Engineering, Toronto, Ontario, Canada, June 3-9, 1990. M. Vijayakumar and S.N. Tewari, Cleveland State University, Chemical Engineering Dept., Cleveland, Ohio 44115; M. Vijayakumar, NASA Resident Research Associate on leave from Defense Metallurgical Research Laboratory, Hyderabad-500258, India. J.E. Lee and P.A. Curreri, NASA Marshall Space Flight Center, Huntsville, Alabama 35812.

16. Abstract

Single crystal specimens of nickel base superalloy PWA-1480 have been directionally solidified on ground and during low gravity (20 sec) and high gravity (90 sec) parabolic maneuver of KC-135 aircraft. Thermal profiles were measured during solidification by two in-situ thermocouples positioned along the sample length. The samples were quenched during either high or low gravity cycles so as to freeze the structures of the mushy zone developing under different gravity levels. Microsegregation has been measured by examining the solutal profiles on several transverse cross-sections across primary dendrites along their length in the quenched mushy zone. Effect of gravity level on secondary arm coarsening kinetics and microsegregation have been investigated. The results indicate that there is no appreciable difference in the microsegregation and coarsening kinetics behavior in the specimens grown under high or low gravity. This suggests that short duration changes in gravity/levels (0.02 to 1.7 g) do not influence convection in the interdendritic region. Examination of the role of natural convection, in the melt near the primary dendrite tips, on secondary arm spacings requires low gravity periods longer than presently available on KC-135. Secondary arm coarsening kinetics show a reasonable fit with the predictions from a simple analytical model proposed by Kirkwood for a binary alloy.

17. Key Words (Suggested by Author(s))	18. Distribution Statement
Superalloy Single crystal Microgravity Microsegregation	Unclassified – Unlimited Subject Category 26

19. Security Classif. (of this report)	20. Security Classif. (of this page)	21. No. of pages	22. Price*
Unclassified	Unclassified	12	A03

NASA FORM 1626 OCT 86

*For sale by the National Technical Information Service, Springfield, Virginia 22161